Articles in PresS. Am J Physiol Heart Circ Physiol (August 4, 2006). doi:10.1152/ajpheart.00259.2006

Frequency-based analysis of the early, rapid-filling pressure-flow relation elucidates diastolic efficiency mechanisms

Yue Wu, Sándor J. Kovács
Cardiovascular Biophysics Laboratory, Washington University,
St. Louis, MO, USA

Short Title: E-wave optimization

Address for correspondence:

Sándor J. Kovács, PhD, MD
Cardiovascular Biophysics Laboratory
Washington University Medical Center
660 South Euclid Ave, Box 8086
St. Louis, MO. 63110
(Phone) (314) 454-8146
(FAX) (314) 454-8250
E-mail: sjk@wuphys.wustl.edu

Abstract

Stiffness- and relaxation-based diastolic function (DF) assessment can characterize the presence, severity and mechanism of dysfunction. Although frequency-based characterization of arterial function is routine (input impedance, characteristic impedance, arterial wave reflection) DF assessment using frequency-based methods incorporating optimization/efficiency criteria are lacking. By definition, optimal filling maximizes (E-wave) volume, minimizes 'loss' at constant stored elastic strain-energy (which initiates mechanical, recoil-driven filling). In thermodynamic terms, optimal filling delivers all oscillatory power (rate of work) at the lowest harmonic. To assess early rapid-filling optimization, simultaneous micromanometric left ventricular pressure (LVP) and echocardiographic transmitral flow (Doppler E-wave) were Fourier analyzed in 31 subjects. A validated kinematic filling model provided closed-form expressions for E-wave contours and model parameters. Relaxation-based DF impairment is indicated by prolonged E-wave deceleration time (DT). Optimization was assessed via regression between the dimensionless ratio of 2nd (*Q2*) and 3rd (*Q3*) flow harmonics to the lowest harmonic (*Q1*), i.e. (*Q2/Q1*) or (*Q3/Q1*) vs. DT or *c*, the filling model's viscosity/damping (energy-loss) parameter. Results show that DT prolongation or increased *c*, generated increased oscillatory power at higher harmonics (*Q2/Q1*=0.00091•DT+0.09837, r=0.70; *Q3/Q1*=0.00053•DT + 0.02747, r=0.60; *Q2/Q1*=0.00614•*c* +0.15527, r=0.91; *Q3/Q1*=0.00396•*c*+0.05373, r=0.87). Because ideal filling is achieved when all oscillatory power is delivered at the lowest harmonic, the observed increase in power at higher harmonics is a measure of filling inefficiency. We conclude that frequency-based analysis facilitates assessment of filling efficiency and elucidates the mechanism by which diastolic dysfunction associated with prolonged DT impairs optimal filling.

Keywords: diastolic function, Fourier analysis, Doppler echocardiography, cardiac catheterization, efficiency

INTRODUCTION

The epidemiologic fact that heart failure (HF) is the most frequent single diagnosis related group for hospitalization (10,14) and that diastolic heart failure, which comprises up to 50% of HF admissions, has reached epidemic proportions (14) has provided added impetus for detailed characterization of all aspects of the physiology of diastole and methods by which diastolic dysfunction can be diagnosed. Hence, investigation of how the heart works when it fills (diastolic function) is proceeding on multiple theoretical and experimental fronts spanning six orders of magnitude, involving molecular, genetic, cellular biologic as well as organ system mechanisms (14). Consensus has developed that for phenotypic characterization of diastolic function (DF) and diastolic dysfunction (DD), the most appropriate measures, in addition to filling (stroke) volume and ejection fraction (EF), are chamber stiffness and relaxation (1,2,14,17).

The concept of pathologic stiffness in cardiovascular physiology is familiar in the context of properties of the arterial circulation (5,19,20). In addition to stiffness of the arterial tree, quantitatively characterized in terms of pressure P and flow Q (or dP/dQ), frequency-based characterization of the periphery achieved by Fourier analysis of the oscillatory pressure and flow waveforms is standard (5,19,20,24). Despite the successful application of Fourier methods in characterizing arterial stiffness, little effort has been made to use similar methods to study the stiffness-related mechanisms of DF or DD. To overcome this limitation, we previously introduced the concept of impedance analysis as a method for DF characterization (28). In precise analogy to frequency-based analysis of pressure and flow applied to the peripheral circulation, our method determined input impedance, characteristic impedance and the reflection coefficient of the left ventricle (LV) by analysis of pressure and flow during early-rapid filling (Doppler E-wave). As anticipated from theoretical and physiologic arguments based on the role of the LV as

a suction- pump, we found that the LV generates a negative reflection coefficient during the E-wave due to the phase difference between pressure and flow. Moreover, filling in normal hearts operates very near the optimal phase angle (*180°*) that minimizes the reflection coefficient (28). The existence of an optimal phase angle (between *P* and *Q*) implies optimization between the dominant (1^{st} harmonic) pressure-wave and flow-wave during early-rapid filling. This is equivalent to maximizing filling volume at a suitably low pressure for a given amount of available stored elastic energy. In support of the hypothesis that normal filling is close to optimal, we found that subjects with DD (elevated LVEDP or delayed relaxation) demonstrated decreased filling efficiency in terms of a phase-shift of their pressure-flow relation relative to normal by having a higher reflection coefficient phase angle, which deviates from its optimal value of *180°* and causes a higher input impedance (28).

In this study, we applied frequency-based analysis to LV pressure (LVP) and flow to further characterize the efficiency related mechanisms of the pressure-flow relationship in early diastole. In analogy to methods previously utilized for characterization of arterial stiffness, although never previously applied for the characterization of DF, we analyzed the relation between Fourier amplitudes as a function of increasing harmonics and measures of DD such as E-wave deceleration time (DT).

MATERIALS AND METHODS

Data Acquisition. Data acquisition has been previously described (28). Briefly, informed consent for participation was obtained from all subjects in accordance with WUMC Human Studies Committee [IRB] guidelines. Thirty-one subjects [age 56±9 years, EF 62±18 %, 19 male] undergoing elective diagnostic cardiac catheterization had simultaneous limb lead II of the

electrocardiogram (ECG), LVP, and transmitral flow velocities recorded. Transthoracic transmitral flow was recorded via an Acuson Sequoia C256 echocardiographic imager (Mountain View, CA) equipped with a 2 MHz transducer, using pulsed Doppler echocardiography. In accordance with ASE criteria (22), the sample volume (3 mm) was located at the mitral leaflet tips using the four-chamber view and the direction of insonification was aligned as parallel as possible to the color Doppler determined transmitral flow direction. Baseline filters were set at the lowest setting. Micromanometric LVP contours from a Millar catheter (Model SPC-560-1, Millar, Houston, TX) were fed to catheterization laboratory amplifier (Quinton Diagnostics, Bothell, WA) for on-site monitoring and the signal was also acquired by Leycom multichannel control unit (Leycom, Netherlands, Model Sigma 5 DF). The precision of the pressure signal is 0.5mmHg. Pressure, volume and ECG signals were A/D converted at 200 Hz and saved to an accompanying data acquisition system. Pressure and ECG were fed into the physiologic auxiliary port of the echocardiography imager for temporal alignment with transmitral flow.

Echocardiographic image analysis. Transmitral flow *Q(t)* (cm^3/sec), i.e. rate of LV volume increase, was defined as the product of Doppler E-wave velocity (cm/sec) and constant effective mitral valve area (cm^2) i.e. velocity•area. To eliminate uncertainties related to Doppler E- and A-wave superposition, only subjects with a diastatic interval or minimal overlapping were considered. For each subject, three beats were selected for analysis and the results were averaged to get time-invariant E-wave parameters. Transmitral flow (E-waves) and pressure contours were temporally aligned and coupled relative to a fiducial square-wave marker in the pressure channel. To achieve additional precision in temporal alignment of pressure and flow data, cardiac cycle timing events were overdetermined by utilizing both the QRS and mitral valve opening and closing features on the echo image. E-wave (flow) data analysis and processing was done on an IBM-PC running a custom-made LabVIEW 6 (National Instruments, Austin, TX) program,

utilizing a previously validated model-based image processing (MBIP) method for LV diastolic function determination (9,13). The MBIP method models the kinematics of filling in analogy to the motion of a simple harmonic oscillator (SHO). The Levenberg-Marquardt algorithm is used to minimize the difference between the model-predicted velocity and the actual E-wave contour to generate the three SHO parameters: c (damping coefficient), k (spring constant), and x_o (initial displacement). These parameters uniquely characterize the rate of decay, frequency, and amplitude of the E-wave. Compared to other echocardiographic indexes which only rely on one or two points of the entire E-wave contour, the MBIP method utilizes nearly all the data points on the contour and concomitantly generates a quantitative measure of goodness of fit (9,21), whose mean squared error is less than 2cm/s. Additionally, the three parameters have well-established physiologic analogues: chamber stiffness as k (16), chamber viscoelasticity/relaxation as c (6) and volumetric load as x_o (15). Related indexes include, peak atrioventricular pressure gradient as kx_o (3) and stored elastic strain-energy to power recoil as $1/2kx_o^2$ (18).

Temporal synchronization accuracy. Because of the rapid increase in pressure at mitral valve closing i.e., start of isovolumic contraction (IVC), the timing of mitral valve closing (end of A-wave) can be easily discerned from $P(t)$, and is synchronized to end of A-wave. The intraobserver variation for alignment of flow to pressure in a given cardiac cycle was determined by comparison of the precision of repeated alignments for the entire set of pressure/flow data over a time interval of two or more weeks. For data sets (E-wave durations) with a typical duration of 250-300ms the accuracy was within 10ms, yielding an intra-observer variation of <5% for pressure-flow alignment for the same beats.

Data processing. As previously described (28), simultaneously acquired and digitized pressure and flow data were subjected to Fourier transform (FT) by the following equation:

$$P^*(\omega_m) = \frac{1}{N}\sum_{0}^{N-1} P(n)e^{-i2\pi mn/N}$$
$$Q^*(\omega_m) = \frac{1}{N}\sum_{0}^{N-1} Q(n)e^{-i2\pi mn/N}, \quad [1]$$

where N is the number of data points of digitized $P(t)$ and $Q(t)$, i.e. $P(n)$ and $Q(n)$ respectively, from mitral valve opening to the end of the E-wave at which mitral valve closes; $\omega_m = 2\pi m f_s/N$; $m,n = 0,1,\ldots,N\text{-}1$; f_s is the data acquisition sampling rate, which is 200Hz in our data acquisition setting. Traditionally, harmonic frequencies are defined as $f_m=\omega_m/2\pi$. Specifically f_1 is called fundamental frequency and defined as f_s/N.

Prediction and Analysis. Considering the concept of work in mathematical terms (defined as: $W=\int(P(t)-P_{LA}(t))\bullet Q(t)dt$, where $P(t)$ is LVP, $P_{LA}(t)$ is left atrial pressure (LAP) and $Q(t)$ is transmitral flow rate), it can be shown that optimal efficiency is achieved when all work is delivered at the fundamental (n=1) frequency, with the approximation that the DC component of $P(t)$ and $P_{LA}(t)$ are indistinguishable (see Discussion). Thus, for a ventricle using stored elastic strain energy to initiate recoil-driven filling, it follows that the optimal state is achieved if all oscillatory components reside at a single (1st) harmonic because of the orthogonality property of the sine function. Hence, whether an oscillatory pressure component at certain frequency ω_n, $[P(\omega_n)sin(\omega_n t)]$, does effective work on an oscillatory flow component at another frequency ω_m, $[Q(\omega_m)sin(\omega_m t)]$, depends on their relative frequencies, i.e. the effective work is $P(\omega_n)\bullet Q(\omega_m)\bullet\delta_{m,n}$, where $\delta_{m,n}$ is defined as:

$$\delta_{m,n} = 1, \quad for\ n = m$$
$$\delta_{m,n} = 0, \quad for\ n \neq m. \quad [2]$$

To achieve optimal filling we predict that higher harmonics (n>1) should be negligible or be close to zero, so that the largest possible contribution of the oscillatory pressure and flow component resides at the lowest frequency, therefore maximizing $\int(P(t)-P_{LA}(t))\bullet Q(t)dt$ for the lowest value of n. The FT of a sinusoid at a fixed frequency yields a single component at that frequency. FT of an oscillatory waveform that deviates from a pure sine wave will generate components of higher frequency than the fundamental, typically with diminishing amplitudes as a function of increasing frequency. The amplitude of each component can be used to compute the amount of oscillatory power at that frequency (19, p.265). To evaluate the contribution of the non-dominant components to the oscillatory power, we normalize the harmonic power relative to the 1st harmonic and define the harmonic power factor in the format of *Qn/Q1* and *Pn/P1*, where *Pn* and *Qn* are the nth harmonic amplitudes of pressure and flow respectively, and *P1* and *Q1* are the 1st harmonic amplitudes of the pressure and flow waveforms respectively.

By determining harmonic power factors above the fundamental (n>1), we can determine efficiency by regressing *Qn/Q1* vs. E-wave deceleration time (DT) or vs. kinematic model derived damping constant *c*. Hence, we can assess whether a Doppler E-wave is indeed optimized in terms of its dependence on oscillatory power.

RESULTS

A typical synchronized pressure and flow tracing as a function of time is shown in Fig. 1(a). The Fourier analysis results for the *P* and *Q* waveforms of early-rapid filling, i.e. amplitudes of DC, 1st to 7th harmonics are shown in Fig. 1(b). There is no physiologic reason to consider frequency content beyond 10 Hz (beyond 3rd harmonic) for the E-wave, therefore we set the cut-off frequency at 10 Hz (28). For clarity, in Fig 1(c) and 1(d), we plotted the harmonic

components of *P* and *Q* from the 1st to 7th harmonics. As anticipated (28), we observed that the lower the harmonic, the higher the amplitude, and, from 5th and greater harmonics, the amplitude contributes less than 5% of the total oscillatory amplitude. Accordingly, the 5th and greater harmonics are deemed negligible. E-waves with longer DTs were associated with broadening of the oscillatory amplitude spectrum at higher harmonics as shown in Fig. 2. The relationship between increased values for the damping parameter *c* and the associated manifestation of more oscillatory power at higher harmonics is shown in Fig. 3. Availability of the Fourier components permits quantitation of the oscillatory power ratio, defined as power, $W(\omega_n) = P(\omega_n) \bullet Q(\omega_n)$, at different harmonics. The relative total power at higher harmonics in terms of the ratio of 2nd and 3rd harmonic power to the 1st, i.e. $(P2 \bullet Q2)/(P1 \bullet Q1)$ and $(P3 \bullet Q3)/(P1 \bullet Q1)$ are shown in Fig. 4. Using the average value of *P2/P1*, *P3/P1*, *Q2/Q1* and *Q3/Q1* in Table 1, we calculated that an ideal E-wave is 12% more efficient than the whole subject set (see Discussion).

DISCUSSION

Consideration of the heart as a pump indicates that it is about 15-18% efficient in mechanical terms when the area of the pressure-volume loop (external work per cardiac cycle) is compared to the potential (chemical) work (A-V O_2 difference) extracted from its arterial supply (20). Although several nonlinear and one linear model of diastolic filling have been proposed (15, 21), no previous work addresses the efficiency of filling (diastole) by itself, either in mechanical or thermodynamic terms. Because kinematic model and other nonlinear models (21) of filling accurately predict E-wave contours, the modeling paradigm itself provides a method by which filling efficiency can be characterized. The essential feature of kinematic modeling of filling is the requirement that the model account for the role of the LV as a mechanical suction pump

(dP/dV <0 at MVO, and briefly thereafter). Filling is viewed as being analogous to a spring (stored, end-systolic elastic strain in tissue) recoiling at mitral valve opening, overcoming the effects of inertia (blood/tissue) and resistance (viscous effects) (9,13). This paradigm yields a linear, invertible filling model that obeys the kinematics of a damped SHO and exploits its parameters. The model determines unique physiologic parameters (i.e. solves the 'inverse problem' of filling) by using the contour of the clinical Doppler transmitral E-wave as input (9,13). The physics of SHO motion, and the availability of solutions for velocity (time derivative of displacement) as a function of time in closed algebraic form naturally leads itself to frequency-based analysis of filling. An idealized, undamped spring has a natural (fundamental) frequency. If the motion is damped (i.e. presence of viscosity), Fourier analysis of the velocity necessarily includes higher oscillatory components (harmonics) at integer multiples of the fundamental frequency. In the absence of damping, all the oscillatory energy is delivered at the fundamental frequency (1st harmonic). In the presence of increasing amounts of damping, the 2nd and higher harmonic components become manifest, and a greater portion of the total oscillatory (potential) energy is distributed among the higher harmonic components. Accordingly, by both kinematic and thermodynamic criteria, an optimal E-wave generated by the rules of SHO motion, and driven by a fixed amount of stored elastic energy ($1/2kx_o^2$ in kinematic model terminology), maximizes filling volume in the time available at physiologic (low) pressures. In the language of kinematic modeling (SHO motion), such an ideal E-wave corresponds to undamped (lossless) motion, equivalent to a negligible value for the damping constant (i.e. $c = 0$). From the perspective of optimization of efficiency (or maximization of work) in frequency terms, the existence of oscillatory power at frequencies higher than the fundamental is the sine qua non of inefficiency because the atrioventricular pressure gradient is dominated by the first harmonic, and sinusoidal functions are orthogonal. The causal, physiologic consequences are, that a given

harmonic of the pressure waveform does work only on the same harmonic of the flow waveform (E-wave) (see below for mathematical details)(19,20). The concept of power optimization can be appreciated by comparing an ideal E-wave and a damped E-wave having the same filling volume. The ideal E-wave $Q_i(t)$ is expressed as $Q_i(\omega_1)sin(\omega_1 t)$, and the damped E-wave $Q_d(t)$ is expressed as $Q_d(\omega_1)sin(\omega_1 t)+ Q_d\ (\omega_2)sin(\omega_2 t)+ Q_d\ (\omega_3)sin(\omega_3 t)$ *etc*, where $Q_i(\omega_1)$, $Q_d(\omega_1)$, $Q_d(\omega_2)$ and $Q_d(\omega_3)$ are the harmonic components of each. $Q_i(\omega_1)= Q_d(\omega_1)+ Q_d(\omega_2)+ Q_d(\omega_3)$ since the filling volume is the same. The amount of work to generate the ideal E-wave is $W_i=P1 \bullet Q_i(\omega_1)$, To generate the damped E-wave the actual amount of work W_{actual} is given by $P1 \bullet Q_d(\omega_1)+ P2 \bullet Q_d(\omega_2)+ P3 \bullet Q_d(\omega_3)$ is required. In quantitative terms the optimization can be expressed as the difference between (ideal work – actual work) divided by actual work, i.e. power optimization η = $(W_i - W_{actual}) / W_{actua}$. Using the data from Table 1, the power optimization η computed according to the above expression is 12% for an ideal E-wave compared to the average actual E-waves for the entire group, i.e. for the same amount of initial energy available for filling ($1/2kx_o^2$ in PDF parameter terms) an ideal or optimized E-wave delivers 12% more PQ power.

Fourier analysis of the pressure waveform during early rapid filling for normal subjects reveals that most of the oscillatory power resides at the first (fundamental) harmonic. In contrast, for subjects with E-waves of 'delayed-relaxation' pattern (DT >220ms), a smaller component of the waveform resides at the first harmonic. Figure 4 illustrates that as DT is lengthened, the ratio of P2Q2 and P3Q3 to P1Q1 rises. When viewed in terms of flow, Figure 3 shows that the ratio of Q2 and Q3 to Q1 also rises as *c*, the model derived viscoelastic/damping constant rises. The higher r values achieved in the regression relations of Figure 3, compared to those achieved in Figure 2 are explained by the ability of the parameter *c* to accurately determine the curvilinear deceleration portion of the E-wave, whereas the DT used in Figure 2 is determined by a straight

line drawn to the curvilinear deceleration portion (2,8), which usually underestimates the actual deceleration time. This is also the reason why the r-value in Figure 5 are higher than that in Figure 4.

This property of redistribution of the relative Fourier amplitudes makes filling less efficient in hearts having greater DT or greater *c*. In our previous work (28), we characterized the hydraulic input impedance and reflection coefficient associated with the filling process. We found that the reflection coefficient R*, a complex number defined as the ratio of the reflected wave to the incident wave in terms of amplitude ratio and phase difference, can be expressed as (19,20,28):

$$R^* = \frac{1 - \frac{Z_C}{Z_1}}{1 + \frac{Z_C}{Z_1}}, \qquad [3]$$

where Z_C is characteristic impedance and Z_1 is input impedance at first harmonic (19,20,28). Reflection is optimized with phase angle very near $180°$ since input impedance is minimized, i.e. the same pressure gradient generates greater flow (28). The reflection optimization with phase angle very near $180°$ occurs in subjects with shorter DT (DT <180ms vs. DT>180ms) (28). Achievement of the optimal value for the reflection coefficient would require no damping during the E-wave, i.e. an E-wave having a perfect sinusoidal shape.

In previous work, we demonstrated the feasibility of applying Fourier analysis to the LV pressure contour during the E-wave, where the pressure at E-wave onset and termination numerically differ. This discontinuity between the beginning and the end of the cyclic pressure signal introduces a small change in the spectrum, especially at high frequencies. This discontinuity accounts for the higher input impedances observed at higher harmonics, i.e. $Z_3 > Z_2 > Z_1$ (27), where Z_n is defined as $Z_n=P(\omega_n)/Q(\omega_n)$. However, the dominant component of the

pressure oscillatory power resides at the fundamental harmonic. Even in the presence of the discontinuity between beginning and end of the pressure signal, previous work has shown that the mean squared error between the raw (discontinuous) pressure signal compared to a reconstructed pressure signal using only the first 3 harmonics is only 1.5% (28), hence the presence of the discontinuity has no discernible effect on the results, Moreover, the largest discrepancy between the raw pressure signal vs. reconstructed first 3 harmonics is at the beginning and end of the transform interval corresponding to the early and late parts of E-wave, which have small flow. This results in a negligible difference to the calculation of overall work during the flow interval. To optimally utilize the available oscillatory pressure, the response of flow at the very same frequency is desired. Ideally, the transmitral flow contour should have the form of a perfect sine wave. However, the observed pressure has less oscillatory power at the 1st fundamental harmonic compared to ideal flow as shown in Fig. 1(a). Recall that it is the pressure gradient between left atrium (LA) and LV that drives transmitral flow (7,11,26). It is possible that Fourier analysis of the gradient, rather than LVP, would cause a systematic offset for the energy at the fundamental frequency, and more closely relate flow harmonics to pressure gradient harmonics. Based on the known features that characterize the temporal behavior of the A-V gradient (7,11,26), and constrained by the availability of only the LV pressure during diagnostic catheterization, rather than both LVP and LAP, and the knowledge that during the E-wave the atrium is passive and is not a harmonic source, the expression for P-Q work is as follows. For mathematical simplicity, we use continuous Fourier transform. The external work during the E-wave is:

$$Work = \int_{-\infty}^{+\infty} (P(t) - P_{LA}(t))Q(t)dt\,, \qquad [4]$$

where $P(t)$ is LV pressure, $P_{LA}(t)$ is LA pressure and $Q(t)$ is transmitral flow. The limits of integration are from mitral valve opening (MVO) to the end of E-wave. (Without loss of

generality or any effect on the total work, we can expand the limits of integration from -∞ to +∞ and pad with 0 beyond the E-wave duration.) The pressure gradient between LV and LA has been previously characterized via modeling (11,26) and experimentally (7). After mitral valve opening, early-rapid filling ensues and the pressure gradient reaches its maximum, then reduces to zero near the peak of the E-wave and then reverses sign to decelerate flow. The (passive) atrial pressure contour is similar in shape to the LV pressure contour, but with a small phase lag (11,26). Hence, the contour of A-V pressure gradient is comparable in amplitude, duration and frequency content to LVP during E-wave (11). The dominant harmonics of LVP spectrum must therefore be very similar to the dominant harmonics of the similarly shaped AV pressure gradient (11) and the dominant FT term of the AV gradient waveform will also reside at the first harmonic. These similarities permit approximating the AV gradient spectrum as the LVP spectrum to the leading order. The work W is well approximated as:

$$Work = \int_{-\infty}^{+\infty} P(t)Q(t)dt - \int_{-\infty}^{+\infty} P_{AVR}Q(t)dt \,. \qquad [5]$$

where P_{AVR} is the mean LAP. Putting the second term aside and considering the Fourier and inverse Fourier transform of $P(t)$ and $Q(t)$:

$$\begin{aligned} P^*(\omega) &= \frac{1}{\sqrt{2\pi}} \int_{-\infty}^{+\infty} P(t) e^{-i\omega \cdot t} dt \\ Q^*(\omega) &= \frac{1}{\sqrt{2\pi}} \int_{-\infty}^{+\infty} Q(t) e^{-i\omega \cdot t} dt \end{aligned} \,, \qquad [6a]$$

$$\begin{aligned} P(t) &= \frac{1}{\sqrt{2\pi}} \int_{-\infty}^{+\infty} P^*(\omega) e^{i\omega \cdot t} d\omega \\ Q(t) &= \frac{1}{\sqrt{2\pi}} \int_{-\infty}^{+\infty} Q^*(\omega) e^{i\omega \cdot t} d\omega \end{aligned} \,. \qquad [6b]$$

By substituting Eq. 6a into Eq. 5, we obtain:

$$Work = \frac{1}{\sqrt{2\pi}}\int_{-\infty}^{+\infty}\int_{-\infty}^{+\infty} P^*(\omega)\, e^{i\omega t}\, d\omega \cdot \frac{1}{\sqrt{2\pi}}\int_{-\infty}^{+\infty} Q^*(\omega')\, e^{i\omega' t}\, d\omega'\, dt - \int_{-\infty}^{+\infty} P_{AVR} Q(t) dt\,. \quad [7]$$

We change the notation ω' to $-\omega'$ in $Q^*(\omega')$ portion, to get:

$$Work = \frac{1}{2\pi}\int_{-\infty}^{+\infty}\int_{-\infty}^{+\infty} P^*(\omega)\, e^{i\omega t}\, d\omega \cdot \int_{+\infty}^{-\infty} Q^*(-\omega')\, e^{-i\omega' t}\, d(-\omega')dt - \int_{-\infty}^{+\infty} P_{AVR} Q(t) dt\,. \quad [8]$$

We bring $Q^*(-\omega')$ and $d(-\omega')$ out of the $\int dt$ integration since they do not explicitly depend on t:

$$Work = \frac{1}{2\pi}\int_{-\infty}^{+\infty} P^*(\omega) d\omega \cdot \int_{-\infty}^{+\infty} \overline{Q^*(\omega')} d\omega \cdot \int_{-\infty}^{+\infty} e^{i(\omega-\omega')t}\, dt - \int_{-\infty}^{+\infty} P_{AVR} Q(t) dt\,. \quad [9]$$

The $\int e^{i(\omega-\omega')t} dt = 2\pi\delta(\omega-\omega')$, as integration defines the delta function (29), to get:

$$Work = \frac{1}{2\pi}\int_{-\infty}^{+\infty} P^*(\omega) d\omega \cdot \int_{-\infty}^{+\infty} \overline{Q^*(\omega')} \cdot 2\pi\delta(\omega-\omega') d\omega' - \int_{-\infty}^{+\infty} P_{AVR} Q(t) dt\,. \quad [10]$$

By applying the property of delta function, we calculate the second integral:

$$Work = \int_{-\infty}^{+\infty} P^*(\omega)\overline{Q^*(\omega)} d\omega - \int_{-\infty}^{+\infty} P_{AVR} Q(t) dt\,. \quad [11]$$

Converting from continuous FT to discrete FT, we get:

$$Work = \sum_{n=0}^{N-1} P^*(\omega_n)\overline{Q^*(\omega_n)} - \int_{-\infty}^{+\infty} P_{AVR} Q(t) dt$$

$$= \sum_{n=1}^{N-1} P^*(\omega_n)\overline{Q^*(\omega_n)} + P^*(0)\overline{Q^*(0)} - \int_{-\infty}^{+\infty} P_{AVR} Q(t) dt\,. \quad [12]$$

Since the average LAP (P_{AVR}) is the same as the DC component (average) of LVP ($P^*(0)$) during E-wave, i.e. $P^*(0) = P_{AVR}$, the second and third terms canceled out. Hence the work done is:

$$Work = \sum_{n=1}^{N-1} P^*(\omega_n)\overline{Q^*(\omega_n)}\,. \quad [13]$$

In summary, we use $P(t)-P_{AVR}$ to approximate the A-V gradient, i.e., we approximate LAP to first order during E-wave as a constant ($=P_{AVR}$). Recall that during the E-wave, the LA and the blood are both passive elements and do not introduce any active frequency components into the A-V gradient. Hence the expression for work can be reasonably approximated by the frequency content of LVP and passive flow, responding to the time-varying pressure.

When summarized, these arguments are in concert with previous results attained by other methods (18,23,28). These results provide further physical justification that why an undamped sine wave shaped E-wave contour is desirable in early rapid filling.

Limitations. In concert with convention, and for simplification, we assumed a constant effective mitral valve area (cm^2) by equating volumetric flow rate (cm^3/sec) with E-wave velocity (cm/sec). This has the potential effect of introducing a small, systematic shift to the amplitudes of all frequency/harmonic terms of the volume waveform. Because MRI and echo measurement of normal mitral valve area (MVA) (4) show that it responds passively to the phasic nature of the pressure-flow relation, the small change affecting volume due to time variation of MVA is always in phase with the pressure-flow relation and should not significantly affect the observed trend in the power spectrum as seen in Figs 2 and 3.

CONCLUSIONS

We characterized the efficiency of LV filling via frequency-based analysis of simultaneous left ventricular pressure and transmitral flow (Doppler E-wave) waveforms. Relative to the amplitude of the fundamental harmonic, which contains the most (oscillatory) power, and relative to controls, subjects having the ‘delayed relaxation’ pattern of transmitral flow had an increased fraction of their oscillatory power reside at higher harmonics. The presence

of oscillatory power at higher frequencies is the sine qua non of decreased filling efficiency, which manifests as a decrement in E-wave filling volume (relative to normal). The results underscore the potential value of filling efficiency-derived indexes as physiology-based measures of diastolic function.

ACKNOWLEDGEMENTS

Supported in part by the Whitaker Foundation, National Institutes of Health (HL54179, HL04023), the Heartland Affiliate of the American Heart Association (0310021Z), the Barnes-Jewish Hospital (BJH) Foundation and the Alan A. and Edith L. Wolff Charitable Trust.

The authors appreciate sonographer Peggy Brown's contribution in acquiring high quality echocardiographic data and the assistance of the BJH Cardiac Catheterization Laboratory Staff in high fidelity LV pressure recording.

References

1. **Appleton CP, and Hatle LK.** The natural history of left ventricular filling abnormalities: Assessment by two-dimensional and Doppler echocardiography. *Echocardiography* 9: 437-457, 1992.

2. **Appleton CP, Hatle LK, and Popp RL.** Relation of transmitral flow velocity patterns to left ventricular diastolic function: New insights from a combined hemodynamic and Doppler echocardiography. *J Am Coll Cardiol* 12: 426-440, 1988.

3. **Bauman L, Chung CS, Karamanoglu M, and Kovács SJ.** The peak atrioventricular pressure gradient to transmitral flow relation: kinematic model prediction with in vivo validation. *J Am Soc Echocardiogr* 17(8):839-44, 2004.

4. **Bowman AW, Frihauf PA, and Kovács SJ.** Time-varying effective mitral valve area: prediction and validation using cardiac MRI and Doppler echocardiography in normal subjects. *Am J Physiol Heart Circ Physiol* 287(4): H1650-7, 2004.

5. **Caro CG, Pedley TJ, Schroter RC, and Seed WA.** *The Mechanics of the Circulation*. Oxford University Press, 1978.

6. **Chung CS, Ajo DM, and Kovács SJ.** The Isovolumic Pressure to Early Rapid Filling Decay Rate Relation: Model-based Derivation and Validation Via Simultaneous Catheterization-Echocardiography. *J of App Physiol* 100:528-534, 2006.

7. **Courtois M, Kovács SJ, and Ludbrook PA.** Transmitral pressure-flow velocity relation. Importance of regional pressure gradients in the left ventricle during diastole. *Circ* 78: 661-671, 1988.

8. **Giannuzzi P, Imparato A, Temporelli PL, de Vito F, Silva PL, Scapellato F, and Giordano A.** Doppler-derived mitral deceleration time of early filling as a strong predictor of pulmonary capillary wedge pressure in postinfarction patients with left ventricular systolic dysfunction. *J Am Coll Cardiol* 23(7):1630-7, 1994.

9. **Hall AF, and Kovács SJ.** Automated method for characterization of diastolic transmitral Doppler velocity contours: early rapid filling. *Ultrasound Med Biol* 20: 107-116, 1994.

10. **Kass DA, Bronzwaer JGF, and Paulus WJ.** What Mechanisms Underlie Diastolic Dysfunction in Heart Failure? *Circ Res* 94:1533-1542. 2004.

11. **Keren G, Meisner JS, Sherez J, Yellin EL, and Laniado S.** Interrelationship of mid-diastolic mitral valve motion, pulmonary venous flow, and transmitral flow. *Circ* 74:36-44, 1986.

12. **Kitzman DW.** Diastolic Dysfunction in the elderly: Genesis and Diagnostic and Therapeutic Implications. *Cardiol Clin* 18: 597-620, 2000.

13. **Kovács SJ, Barzilai B, and Pérez JE.** Evaluation of diastolic function with Doppler echocardiography: the PDF formalism. *Am J Physiol Heart Circ Physiol* 252: H178-187, 1987.

14. **Kovács SJ (ed.).** Diastolic Function and Dysfunction, *Cardiol Clin* 18: 411-669, W.B. Saunders, 2000.

15. **Kovács SJ, Meisner JS, and Yellin EL.** Modeling of Diastole. *Cardiol Clin* 18: 459-490, W.B. Saunders, 2000.

16. **Lisauskas JB, Singh J, Bowman AW, and Kovács SJ.** Chamber properties from transmitral flow: prediction of average and passive left ventricular diastolic stiffness. *J of App Physiol* 91: 154-162, 2001.

17. **Little WC, Ohno M, Kitzman DW, Thomas JD, and Cheng CP.** Determination of left ventricular chamber stiffness from the time for deceleration of early left ventricular filling. *Circ* 92(7):1933-9. 1995.

18. **Meyer TE, Kovács SJ, Ehsani AA, Klein S, Holloszy JO, and Fontana L.** Long-term caloric restriction ameliorates the decline in diastolic function in humans. *J Am Coll Cardiol* 47(2):398-402, 2006.

19. **Milnor WR.** *Hemodynamics*. Baltimore, MD: Williams & Wilkins, 1982.

20. **Nichols WW, and O'Rourke MF.** *McDonald's Blood Flow in Arteries: theoretical, experimental and clinical principles.* New York, NY: Oxford university press, 1998.

21. **Nudelman SP, Hall AF, and Kovács SJ.** Comparison of diastolic filling models and their fit to transmitral Doppler contours. *Ultrasound Med Biol* 21(8):989-999, 1995.

22. **Quinones MA, Otto CM, Stoddard M, Waggoner A, and Zoghbi WA.** Recommendations for quantification of Doppler echocardiography: a report from the Doppler Quantification Task Force of the Nomenclature and Standards Committee of the American Society of Echocardiography. *J Am Soc Echocardiogr* 15(2):167-84. 2002.

23. **Riordan MM, Chung CS, and Kovács SJ.** Diabetes and diastolic function: stiffness and relaxation from transmitral flow. *Ultrasound Med Biol* 31(12):1589-96, 2005.

24. **Segers P, Georgakopoulos D, Afanasyeva M, Champion HC, Judge DP, Millar HD, Verdonck P, Kass DA, Stergiopulos N, and Westerhof N.** Conductance catheter-based

assessment of arterial input impedance, arterial function, and ventricular-vascular interaction in mice. *Am J Physiol Heart Circ Physiol* 288(3):H1157-64, 2005.

25. **Sun Y, Sjoberg BJ, Ask P, Loyd D, and Wranne B.** Mathematical model that characterizes transmitral and pulmonary venous flow velocity patterns. *Am J Physiol Heart Circ Physiol* 268(1 Pt 2):H476-89. 1995.

26. **Thomas JD, Newell JB, Choong CY, and Weyman AE.** Physical and physiological determinants of transmitral velocity: numerical analysis. *Am J Physiol Heart Circ Physiol* 260(5 Pt 2):H1718-31, 1991.

27. **Wu Y, Bowman AW, Chung C, Karamanoglu M, and Kovács SJ.** Frequency-Based Analysis of diastolic function. 25th Annual International IEEE-EMBS Conference Proceedings, 2003.

28. **Wu Y, Bowman AW, and Kovács SJ.** Frequency-Based Analysis of Diastolic Function: The Early Rapid Filling Phase Generates Negative Intraventricular Wave Reflections. *Cardiovas Eng* 5(1):1-12, 2005. http://www.springerlink.com/link.asp?id=k6423866850181g8

29. **Zettili N.** *Quantum Mechanics: Concepts and Applications.* pp. 629-631. John Wiley & Sons, LTD, UK. 2001.

FIGURE LEGENDS

Figure 1. A) Typical, simultaneously acquired, digitized waveforms of left ventricular pressure and transmitral flow as a function of time for one cardiac cycle having a duration of 900 msec, equivalent to a heart rate of 66 beats/min. The E-wave contour is obtained via Model-Based Image Processing of the Doppler E-wave image. Only the ~300 msec interval from mitral valve opening (MVO) to diastasis is subjected to Fourier analysis. B) Fourier transform results for the ~300 msec early-rapid filling segment of panel A is shown as (normalized) Fourier amplitude vs. frequency. Note rapid decline in amplitude for increasing harmonics. The decrease of flow harmonic amplitude at higher harmonics relative to the first is faster than that of LVP. C) LVP and first seven harmonic components plotted on the same scale. D) Transmitral E-wave and first seven harmonic components. See text for details.

Figure 2. The relation between 2nd and 3rd oscillatory flow harmonics relative to the fundamental (*Q1*) and E-wave deceleration time (DT). Longer DT indicates worse diastolic function. *Q1*, *Q2* and *Q3* are the E-wave Fourier amplitudes at 1st (fundamental), 2nd and 3rd harmonics. Note r-values and monotonic increase in amplitude ratios with prolongation of DT, indicative of less efficient filling. See text for details.

Figure 3. The relation between 2nd and 3rd oscillatory flow harmonics relative to the fundamental (*Q1*) and kinematic filling model-derived damping constant *c*. We expect relationships similar to those of Fig 2. Larger values of *c* account for longer DT and indicates worse diastolic function. *Q1*, *Q2* and *Q3* are the E-wave Fourier amplitudes at 1st (fundamental), 2nd and 3rd harmonics. Note monotonic increase in amplitude ratios with increased values for *c*, indicative of less efficient filling. Note r-values in Figure 3 are higher than those in Figure 2. See text for details.

Figure 4. The power ratio defined by $P \bullet Q$ at 2nd and 3rd harmonic relative to the 1st harmonic is plotted as a function of DT. Relatively greater power at higher harmonics (2nd and 3rd) is positively correlated with DT and indicates decreased efficiency. The regression relations are: (P2•Q2)/(P1•Q1) = 0.01213+0.00094•DT, r = 0.58 and (P3•Q3)/(P1•Q1) = -0.01233+0.00038•DT, r = 0.54 See text for details.

Figure 5. The power ratio defined by $P \bullet Q$ at 2nd and 3rd harmonic relative to the 1st harmonic is plotted as a function of the kinematic filling model-derived damping constant c. Relatively greater power at higher harmonics (2nd and 3rd) is positively correlated with c and indicates decreased efficiency. The regression relations are: (P2•Q2)/(P1•Q1) = 0.0751+0.0062c, r = 0.74 and (P3•Q3)/(P1•Q1) = 0.0150 + 0.0024c, r = 0.66. Note r-values in Figure 5 are higher than those in Figure 4. See text for details.

Table I: Study Group Characteristics

INDEX	Mean±STD	Range
CLINICAL/HEMODYNAMIC		
Age (yr)	56±9	41–73
gender	19 male/12 female	
LVEF (%)	62±18	17–86
BP_{sys} (mmHg)	131±20	95–175
BP_{dias} (mmHg)	73±12	54–97
HR (bpm)	66±8	53–85
LVEDP (mmHg)	23±7	10–36
Tau (ms)	70±36	35–157
ECHOCARDIOGRAPHIC		
AT (ms)	78±16	43–124
DT (ms)	192±53	91–318
x_o*(cm)*	11±5	-26 – -5
c (gm/sec)	19±10	3.5–44.9
k (gm/sec^2)	227±70	127–463
FREQUENCY-BASED		
P2/P1	0.69±0.16	0.36–1.11
P3/P1	0.45±0.12	0.23–0.80
Q2/Q1	0.27±0.07	0.16–0.44
Q3/Q1	0.13±0.05	0.05–0.25
P2*Q2/P1*Q1	0.19±0.08	0.08–0.49
P3*Q3/P1*Q1	0.06±0.04	0.01–0.20

LVEF: left ventricular ejection fraction; BP_{sys} and BP_{dias}: systolic and diastolic arterial pressure; HR: heart rate; LVEDP: Left ventricular end-diastolic pressure; Tau: time constant of isovolumic relaxation; AT: acceleration-time; DT: deceleration-time; x_o, *c, k*: MBIP model-generated E-wave parameters; P2/P1 (P3/P1): ratio of 2nd (3rd) harmonic pressure- amplitude to fundamental/1st harmonic pressure-amplitude. Q2/Q1 (Q3/Q1): ratio of 2nd (3rd) harmonic flow-amplitude to fundamental/1st harmonic flow-amplitude.

Figure 1

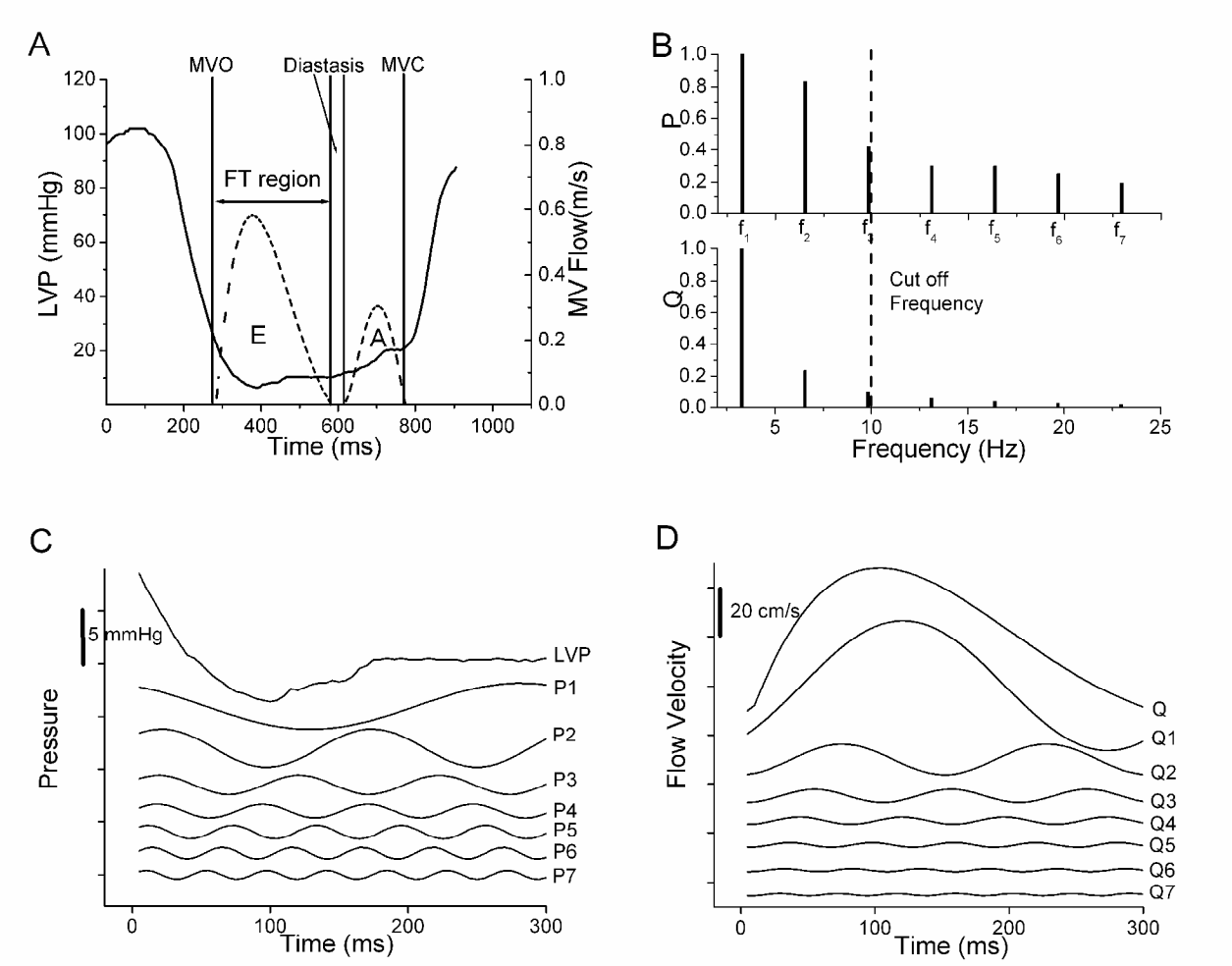

Figure 2

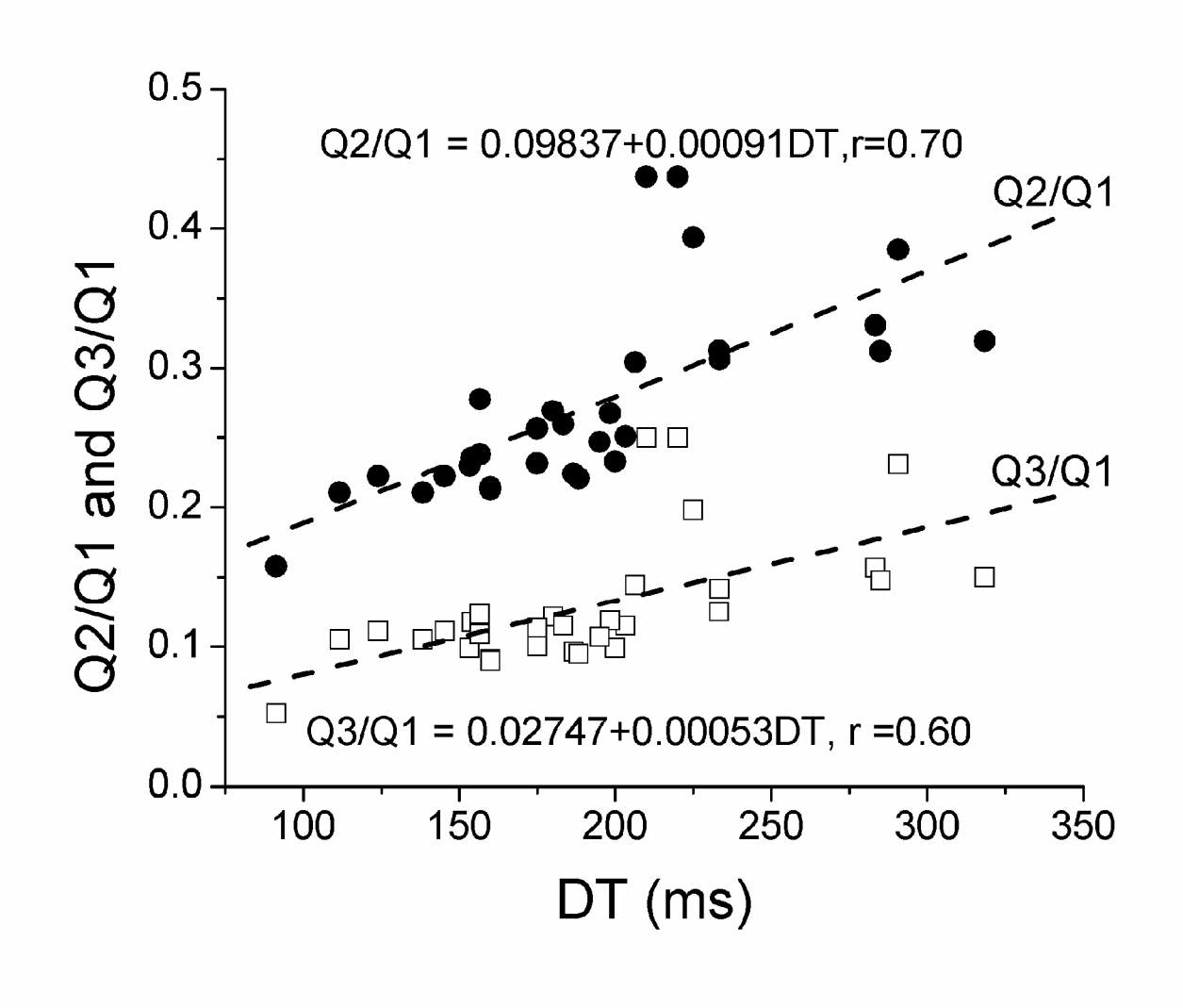

Figure 3

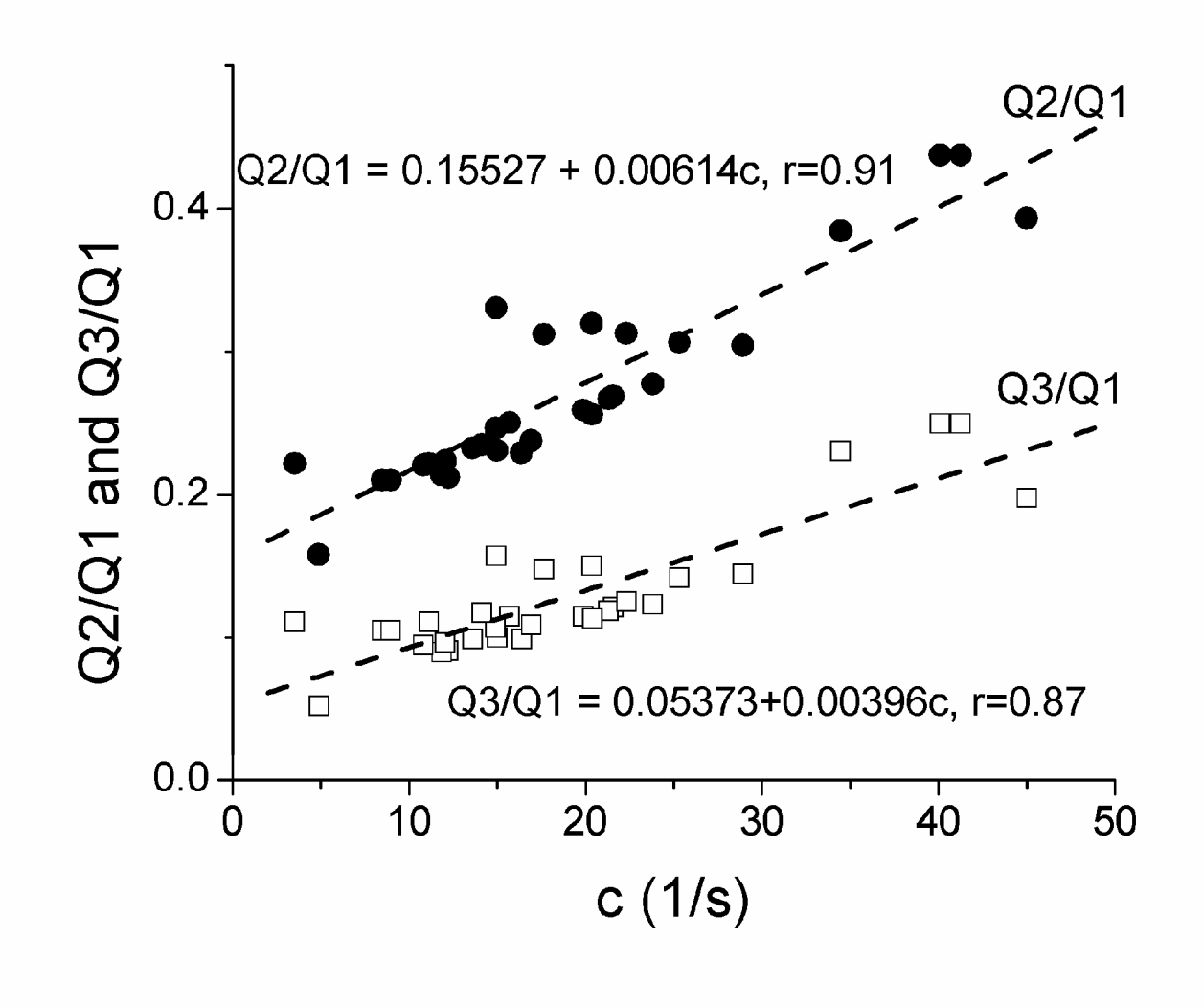

Figure 4

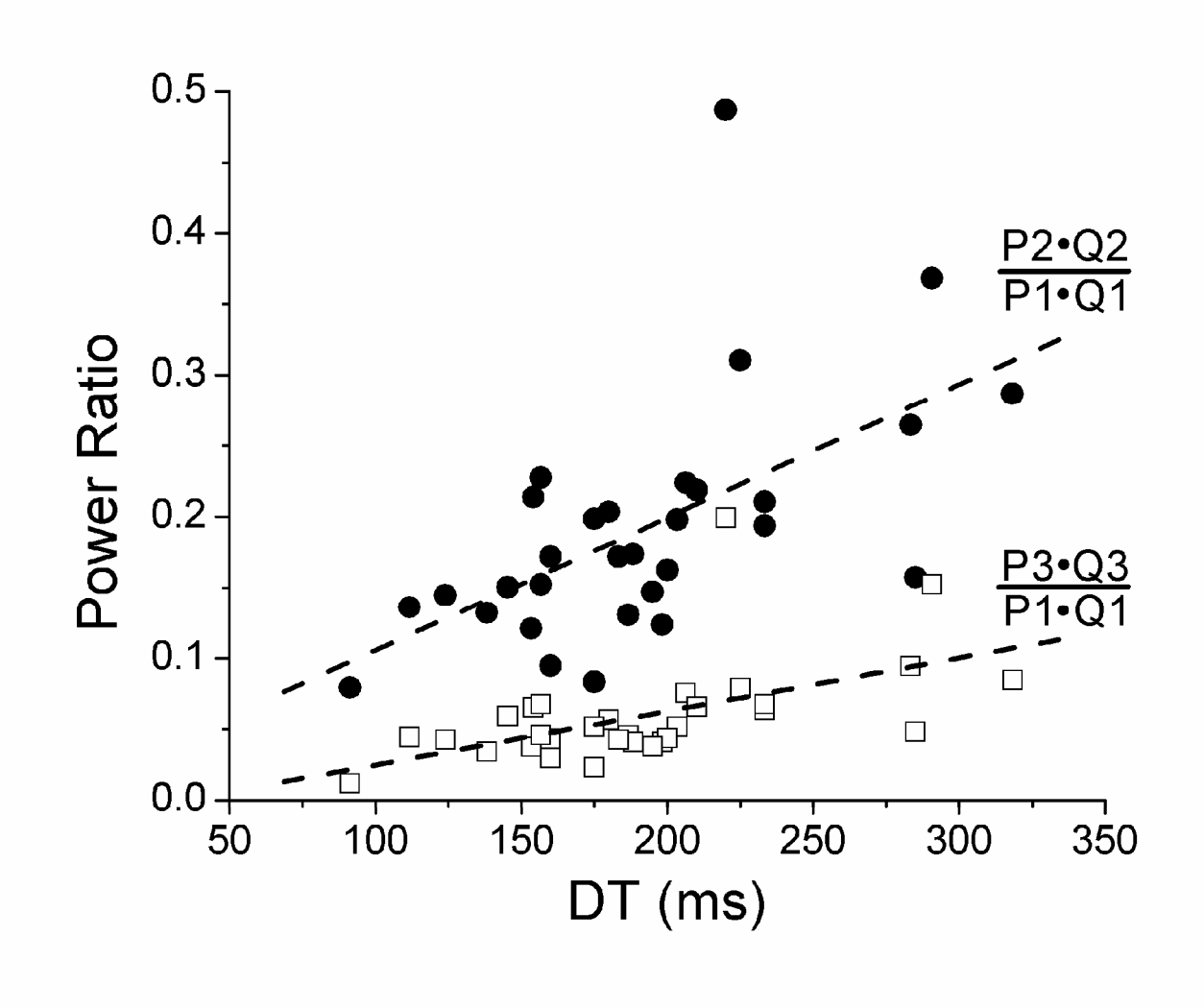

Figure 5